JOURNAL OF MATERIALS SCIENCE 29 (1994) 1773–1780

Effects of crystallization rates on interface layer thickness of epitaxial HDPE on oriented iPP

SHOUKE YAN, JIAN LIN, DECAI YANG
Polymer Physics Laboratory, Changchun Institute of Applied Chemistry, Changchun 130022, People's Republic of China
J. PETERMANN
Department of Chemical Engineering, Dortmund University D-44221, Dortmund, Germany

The effect of crystallization rate on the epitaxial interface layer thickness of high-density polyethylene (HDPE) in the epitaxial system with oriented isotactic polypropylene (iPP) has been investigated by electron microscopy. The results of bright-field electron microscopy and electron diffraction indicate that the epitaxial growth of HDPE on iPP takes place only on the interface between them. The thickness of the epitaxial layer of HDPE is markedly affected by the crystallization rate of HDPE. The critical layer thickness of epitaxial HDPE is about 100 nm under slow crystallization conditions, e.g. isothermal crystallization at 124 °C. When the crystallization rate is higher (quenching into air at room temperature), the epitaxial layer thickness of HDPE increases up to 250 nm.

1. Introduction

In recent years, there has been considerable interest in epitaxial crystallization of crystalline polymers. Generally, the epitaxy of polymers can be divided into two categories, i.e. homoepitaxy and heteroepitaxy. Heteroepitaxy between isotactic polypropylene (iPP) and high-density polyethylene (HDPE), with their chain directions about 50° apart, has been of particular interest because of both the unusual crystalline morphology and the synergism of their mechanical properties [1–3]. A number of publications have appeared on its morphology [4–9]. Their epitaxial relationship has been explained in terms of the alignment of the zig-zag chains along methyl group rows of iPP with 0.5 nm intermolecular distances for a chain-row matching [10, 11]. Very recently, some new epitaxial polymer systems, such as iPP-sPS (PS = polystyrene) and PE-sPP, with different epitaxial relationship, have been reported [12, 13]. The results show that the matching of certain lattice planes may not be the primary factor for the occurrence of epitaxy between polymers. Therefore, it is very important to study the controlling factor of epitaxial crystallization of polymers.

The purpose of this work was to study the effects of some factors, such as crystallization rates and sample thickness, on the epitaxial crystallization of HDPE on iPP by means of electron microscopy and electron diffraction.

2. Experimental procedure

The polymers used in this work were isotactic polypropylene, type Novolene, and polyethylene, type Lupolen 6021 DX, both from BASF AG Ludwigshafen, Germany. Uniaxially oriented thin films of iPP and HDPE were prepared according to a technique reported by Petermann and Gohil [14]. According to this method, a small amount of a 0.5 % solution of the polymer (iPP or HDPE) in xylene was poured and spread on a preheated glass slide where the solvent was allowed to evaporate. After evaporation of the solvent, the remaining thin polymer film was then picked up on a motor-driven cylinder with a drawing speed of $\sim 20\ cm\ s^{-1}$. The temperatures for preparing the melt-drawn films of iPP and HDPE were 140° and 125 °C, respectively. The resulting highly oriented films, which were about 30 nm thick, were mounted on copper grids and directly used for electron microscope observation. For multilayered films of HDPE with iPP, the thin HDPE films were floated on to the surface of distilled water and mounted on top of the iPP substrate film supported by the grids. The thickness of the HDPE layer in the HDPE-iPP system was controlled by putting a different number of HDPE layers on top of the iPP substrate. The HDPE-iPP multilayered films were heated to 150 °C for 10 min and subsequently cooled at different rates to various crystallization temperatures of HDPE. A Joel–2000EX electron microscope operated at 100 kV was used in this study. Bright-field (BF) electron micrographs were obtained by defocus of the objective lens.

3. Results and discussion

3.1 Microstructure of highly oriented iPP and HDPE films

Fig. 1a shows a BF electron micrograph of the iPP substrate film. The arrow in the micrograph indicates

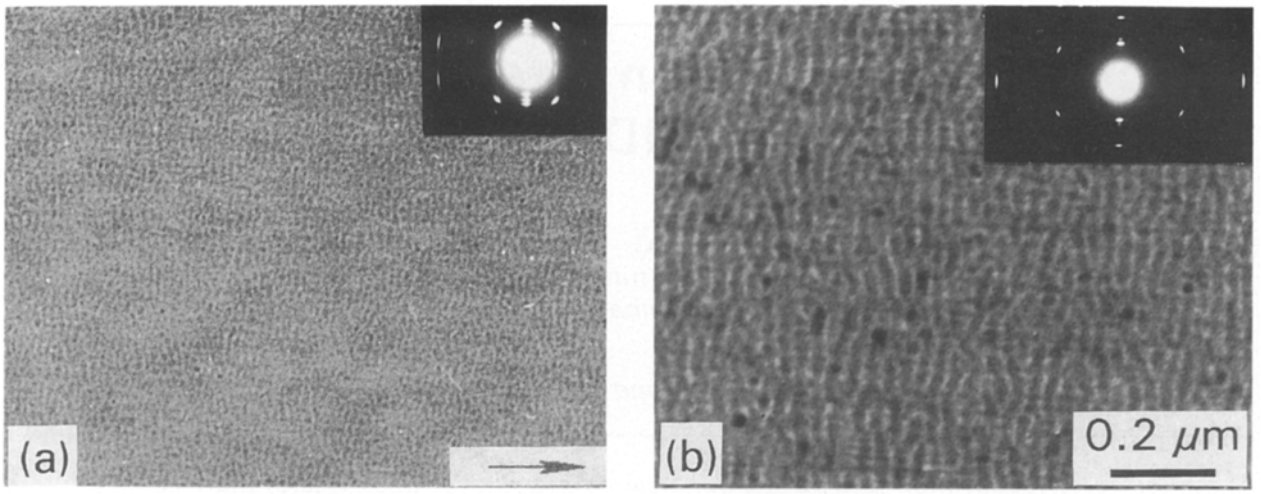

Figure 1 Transmission electron micrographs of (a) iPP substrate film, and (b) oriented HDPE film. The molecular directions are indicated by an arrow.

the drawing direction of the film. On the BF image, small lamellae of iPP are visible which are aligned with their *c*-axes along the drawing direction of the film. The corresponding electron diffraction pattern (insert in Fig. 1a) reveals a high degree of chain-axis orientation.

The BF electron micrograph of HDPE films (shown in Fig. 1b) shows that the HDPE film consists of oriented lamellae and needle crystals, i.e. shish-kebab morphology (with rather low shish content). The electron diffraction pattern (inserted in Fig. 1b) indicates a high degree of crystalline orientation with the *c*-axis

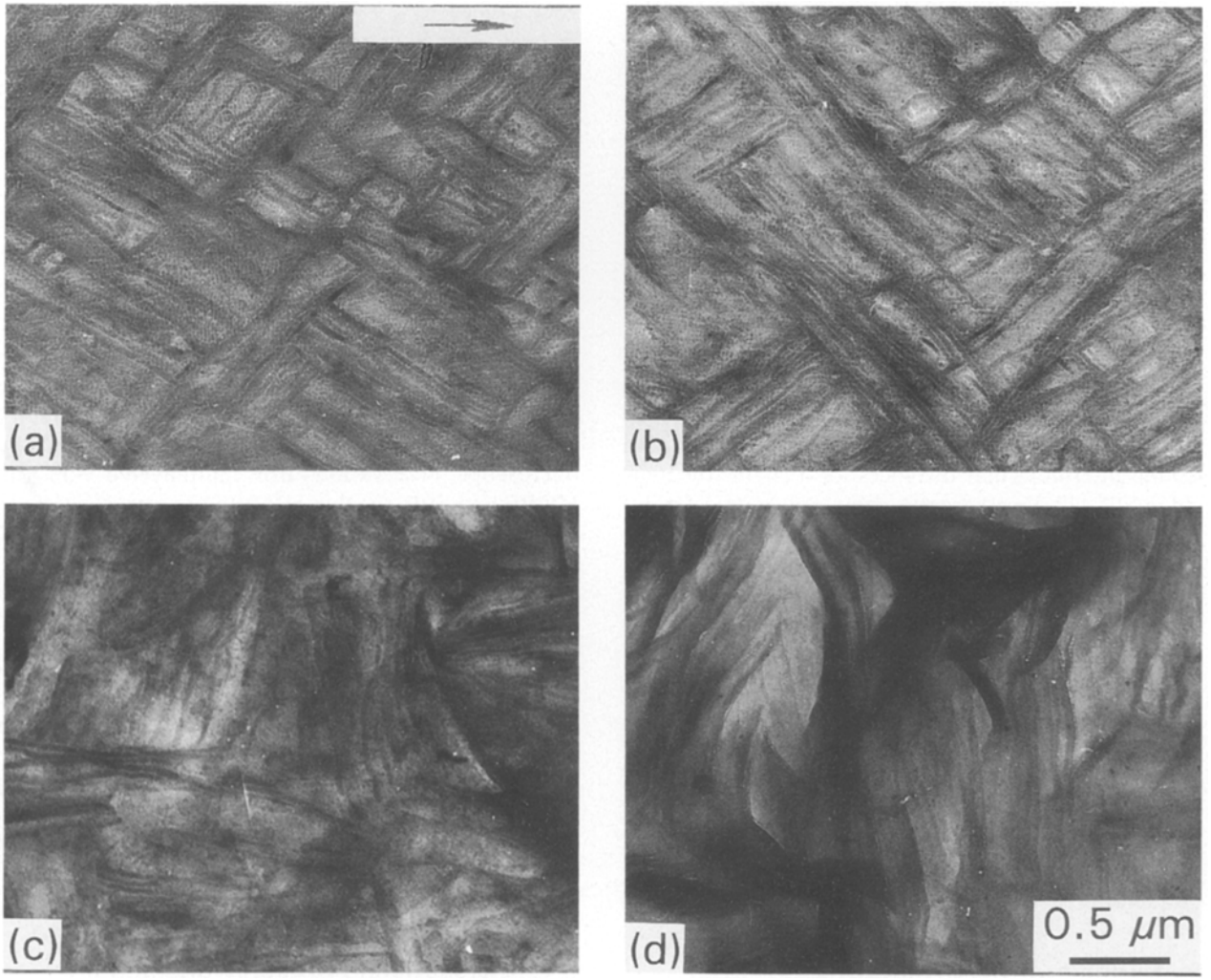

Figure 2 BF electron micrographs of HDPE-iPP multilayered films, heat treated at 150 °C for 10 min and subsequently isothermally crystallized at 124 °C for 5 h, with a thickness of the HDPE layer of (a) 30, (b) 100, (c) 120, and (d) 150 nm, respectively. The arrow shows the iPP chain direction.

parallel to the drawing direction and the *a*-axis perpendicular to the film plane [15].

3.2. Epitaxial crystallization of HDPE on iPP at lower crystallization rates

Fig. 2 shows the electron micrographs of HDPE-iPP multilayered films which were heat treated at 150 °C for 10 min, cooled at 0.5 °C min^{-1} to 124 °C, then isothermally crystallized at this temperature for 5 h, and finally cooled to room temperature. The thickness of the HDPE layer on the iPP substrate is 30, 100, 120 and 150 nm, respectively. The molecular direction of iPP substrate films in the picture is horizontal (as indicated by an arrow). It can be seen that when the thickness of HDPE is thinner than 100 nm (Fig. 2a and b), a cross-hatched lamellar structure arises with the HDPE lamellae being inclined at $\pm 40°$ with respect to the iPP *c*-axes. The average thickness and length of HDPE lamellae are about 40 and 2000 nm, respectively. They do not change much with increase in the thickness of the HDPE layer. The peculiar arrangement of the HDPE lamellae was explained with an epitaxial crystallization of HDPE on oriented iPP substrate [10, 11]. When the thickness of HDPE is thicker than 100 nm, however, crystalline aggregates of HDPE which have no epitaxial relationship with iPP are observed (see Fig. 2c and d). This indicates that there exists a critical epitaxial layer thickness of HDPE on the iPP film, i.e. the epitaxy of HDPE on iPP substrate film can only take place in the interface layer. If the thickness of the HDPE layer is thicker than the critical thickness of the epitaxial layer, no epitaxial orientation relationship between HDPE and iPP lamellae can be observed on the BF images.

Fig. 3 shows the corresponding electron diffraction patterns of the multilayered HDPE-iPP films (heat treated as in Fig. 2). The molecular direction of iPP is indicated by an arrow. It is quite clear from the diffraction patterns that the HDPE, which is thinner

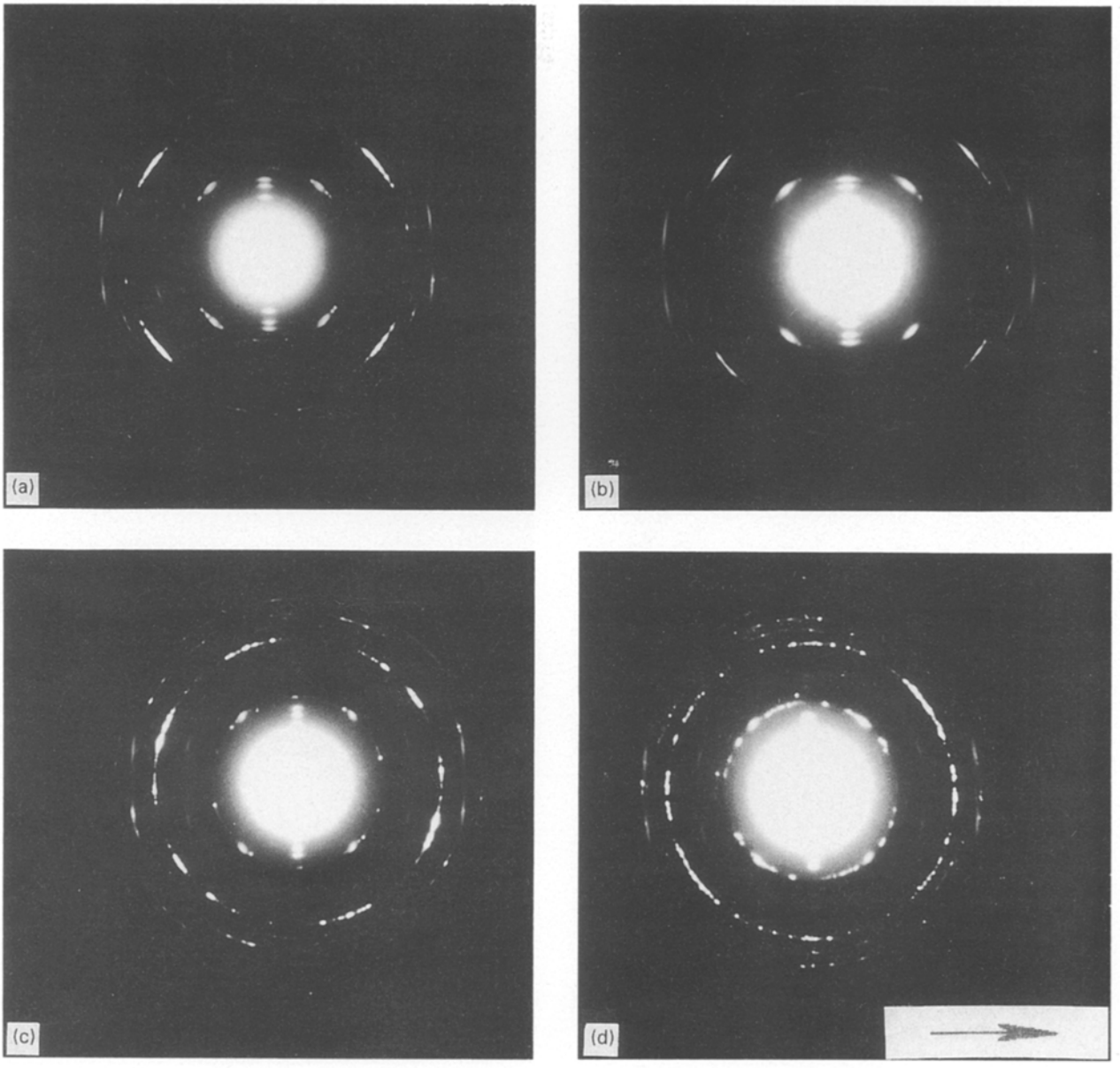

Figure 3 The corresponding electron diffraction patterns of HDPE-iPP multilayered films as in Fig. 2. The arrow represents the iPP chain direction.

than 100 nm (Fig. 3a and b), grows epitaxially on the oriented iPP substrate film with the c-axes inclined at $\pm 50°$ to the c-axes of iPP. The contact planes of the two kinds of crystal are (0 1 0) for iPP and (1 0 0) for HDPE. With increase in thickness of the HDPE layer in the HDPE-iPP system, the (0 2 0) reflections of HDPE change from diffraction points to a discontinuous Debye–Scherrer ring (Fig. 3c). This indicates that there is no epitaxial orientation relationship of HDPE lamellae on the iPP film. This is consistent with the BF observation (Fig. 2c). When the thickness of HDPE was over 150 nm, in addition to the (0 2 0) diffraction ring, a strong (1 1 0) Debye–Scherrer ring of HDPE crystals was observed (Fig. 3d).

Fig. 4 shows BF electron micrographs of HDPE-iPP multilayered films heat treated at 150 °C for

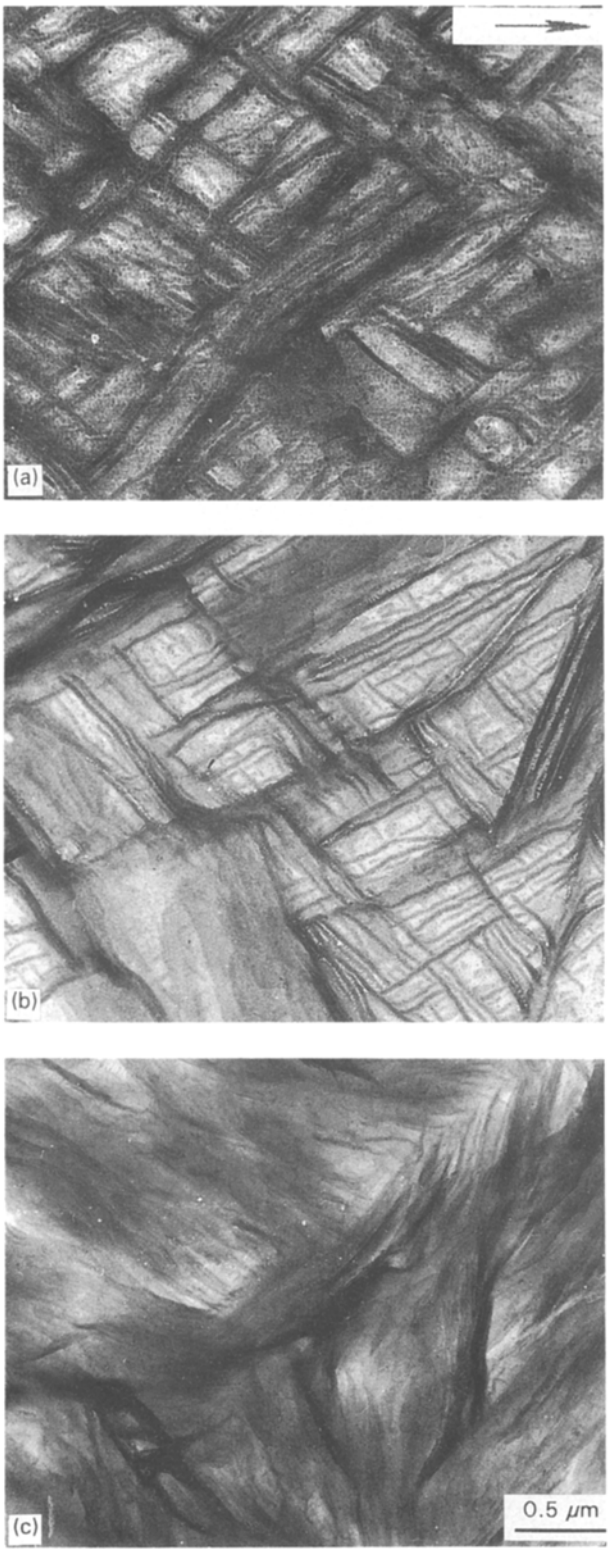

Figure 4 BF electron micrographs of HDPE-iPP multilayered films, heat treated at 150 °C for 10 min and then cooled slowly (at a rate of 0.5 °C min^{-1}) to room temperature. The thickness of the HDPE layer is (a) 60, (b) 120, and (c) 150 nm, respectively.

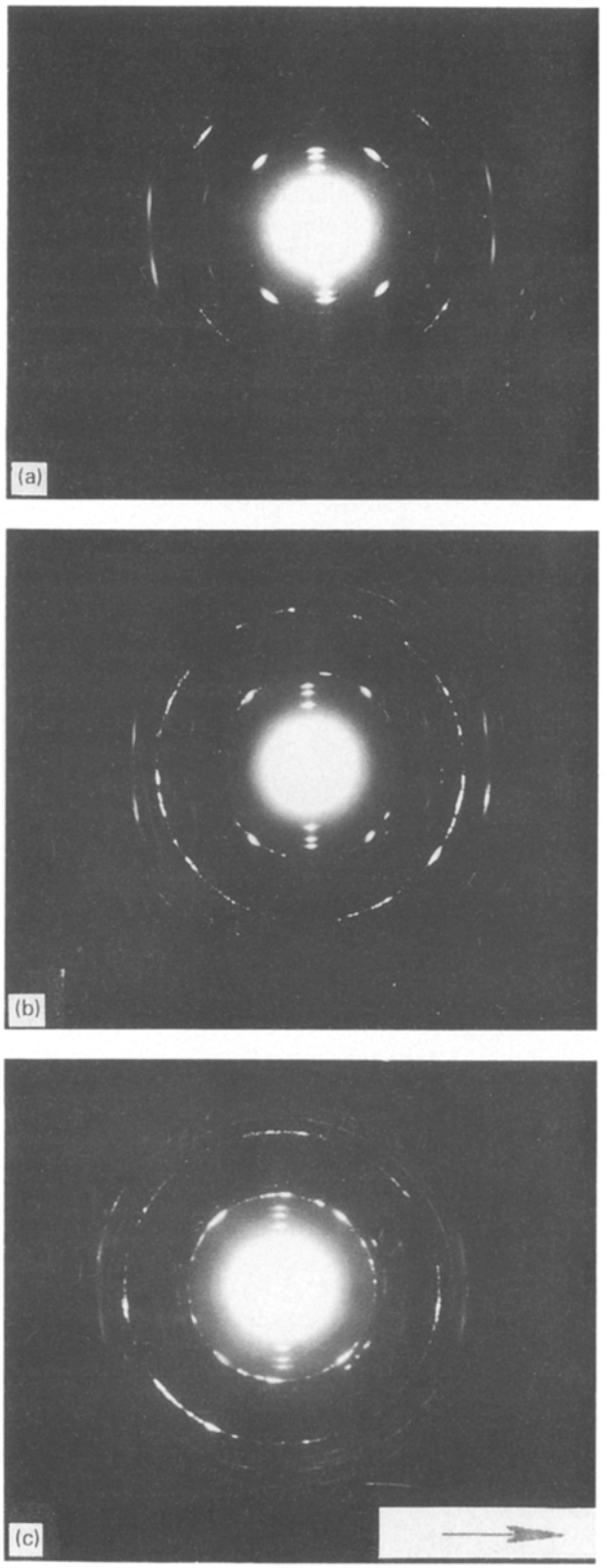

Figure 5 The corresponding electron diffraction patterns of HDPE-iPP multilayered films, as in Fig. 4.

10 min and subsequently cooled slowly (at 0.5 °C min^{-1}) to room temperature. The morphology of recrystallized HDPE is similar to that isothermally crystallized at 124 °C (compare Fig. 4 with Fig. 2). The only difference is that, when the thickness of HDPE layer is about 120 nm, two kinds of crystalline morphology, i.e. lamellae epitaxially grown on the iPP substrate and the crystalline aggregates which have no epitaxial orientation (compare Fig. 4b with Fig. 2c), were observed. The electron diffraction results (Fig. 5) of the layered films are consistent with that isothermally crystallized at 124 °C.

Combining the above results of BF and electron diffraction investigations, a model of the recrystallization process of HDPE on oriented surface of iPP may be suggested (Fig. 6). During the isothermal crystallization (or slow cooling) process, generally, three layers of HDPE crystals are formed. The first layer (in direct contact with the iPP surface) consists of cross-hatched lamellae grown epitaxially on oriented iPP substrate. The growth direction of the HDPE lamellae is along its *b*-axes, and the thickness of the epitaxial layer (the first layer in Fig. 6) should be equal to the lamellar width along the *a*-axes. It is the width that determines the thickness of epitaxial layer of HDPE. If the thickness of the HDPE layer is thinner than the thickness of the critical epitaxial layer, e.g. 100 nm in isothermal crystallization at 124 °C, almost all of the HDPE grows epitaxially on the iPP surface. If the thickness of the HDPE layer is thicker than the thickness of the critical epitaxial layer, e.g. 120 nm, the second crystal layer of HDPE is formed. The second layer mainly consists of oriented crystalline aggregates (see Figs 2c and 4b), which is further confirmed by the results of electron diffraction. The occurrence of the strong Debye–Scherrer ring of the (0 2 0) reflection of HDPE (see Figs 3c and 5b) implies a crystallographic orientation of the crystalline aggregates, with their *a*-axes perpendicular to the film surface, *b*- and *c*-axes in the film plane, but with random orientation. Unambiguously, the nucleation and

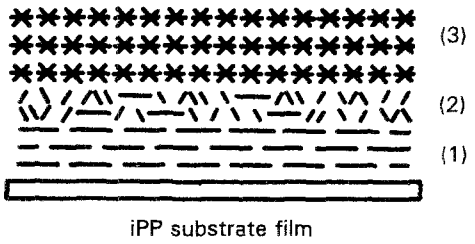

Figure 6 Model of crystallization of HDPE on iPP substrate film at lower crystallization rates. (1) epitaxial HDPE layer, (2) oriented crystalline aggregates, and (3) HDPE spherulite layer.

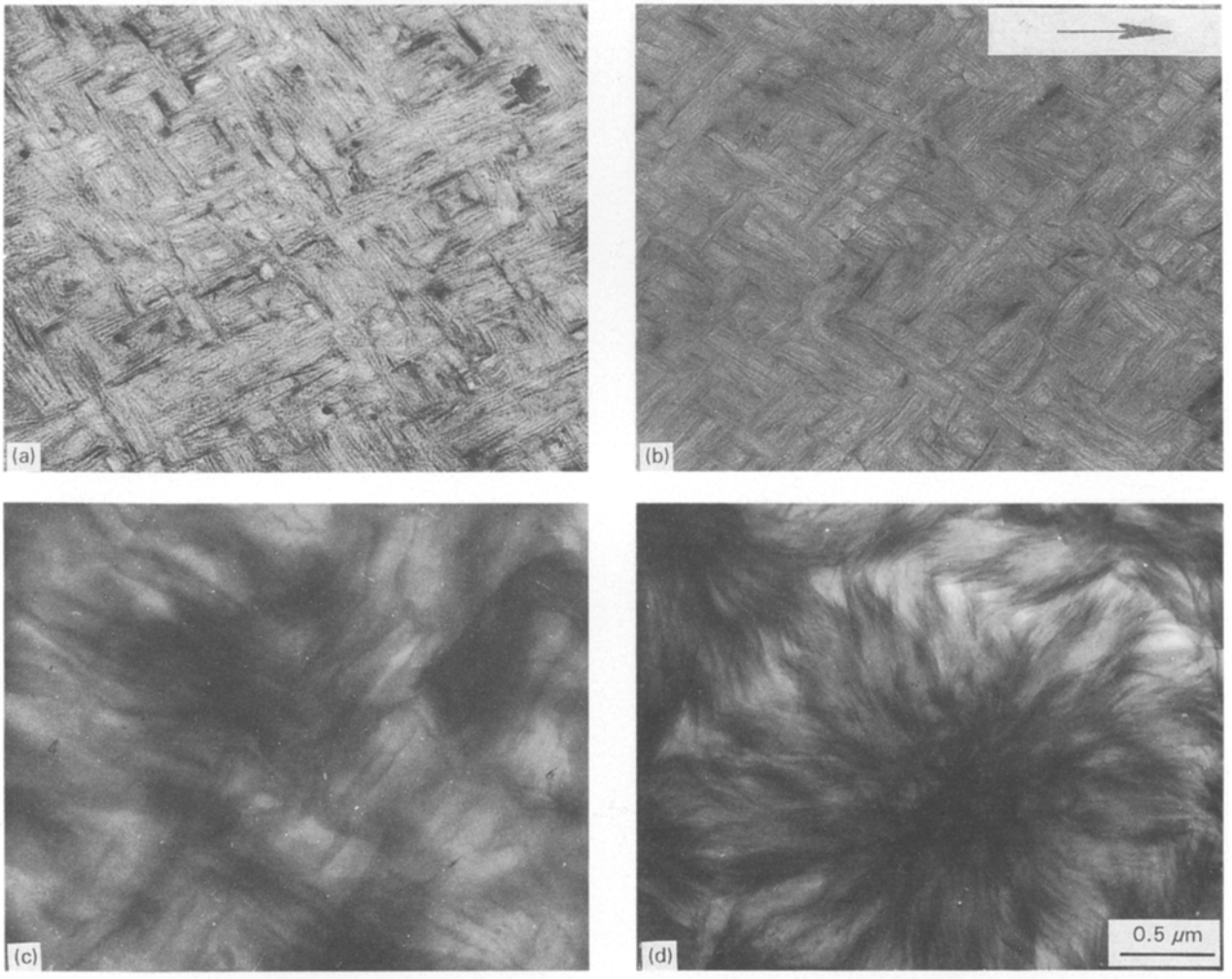

Figure 7 BF electron micrographs of HDPE-iPP multilayered films, heat treated at 150 °C for 10 min and then quenched to room temperature. The thickness of the HDPE layer is (a) 150, (b) 250, (c) 350, and (d) 500 nm, respectively.

growth of the crystalline aggregates take place on the epitaxial layer (the first layer) of HDPE. However, the molecular mechanism for the formation of the oriented (but not epitaxial) crystalline aggregates is not clear now. If the thickness of the HDPE layer is thick enough, e.g. over 150 nm, the third layer, spherulites, is formed (see Figs 2d and 4c). The appearance of the (1 1 0) Debye–Scherrer ring of HDPE in the electron diffraction pattern is a good verification of this (see Figs 3d and 5c).

3.3. Epitaxial crystallization of HDPE on iPP at high crystallization rates

Fig. 7 shows the electron micrographs of HDPE-iPP layered films which have been heat treated at 150 °C for 10 min and subsequently quenched into air at room temperature. The thickness range of the HDPE layer is from 150–500 nm. The molecular direction of iPP is indicated by an arrow in the micrographs. It can be seen that fast quenching results in the formation of smaller HDPE lamellae. The average thickness and length of HDPE lamellae are about 20 and 500 nm, respectively (Fig. 7a and b).

According to the structure relationship revealed in Fig. 7a and b, it is clear that under the present experimental conditions, the thickness of the epitaxial interface layer of HDPE, approximately 250 nm, is much thicker than that at a lower crystallization rate. When the thickness of the HDPE layer is above 250 nm, crystalline aggregates with random orientation or complete spherulites of HDPE are formed (Fig. 7c and d).

The corresponding electron diffraction patterns are presented in Fig. 8. Obviously, the HDPE lamellae grow epitaxially on iPP substrate film when the thickness of HDPE is thinner than 250 nm (Fig. 8a and b). It should be pointed out that when the thickness of HDPE is about 250 nm, in addition to the strong (0 2 0) reflection of HDPE, there exists a weak (1 1 0) Debye– Scherrer ring of HDPE crystals (Fig. 8b). This indicates that most of the HDPE has epitaxially crystallized on the iPP substrate film, but there is a small amount of HDPE crystals which has no orientation relationship with the *c*-axes of iPP crystals. Therefore, the thickness of the epitaxial interface layer or critical epitaxial layer under this condition is near 250 nm. This result is consistent with the BF observation. When the thickness of the HDPE layer is more than that of the critical epitaxial layer, a (1 1 0) Debye–Scherrer ring, which represents the characteristic HDPE spherulite, is seen (Fig. 8c). However, the

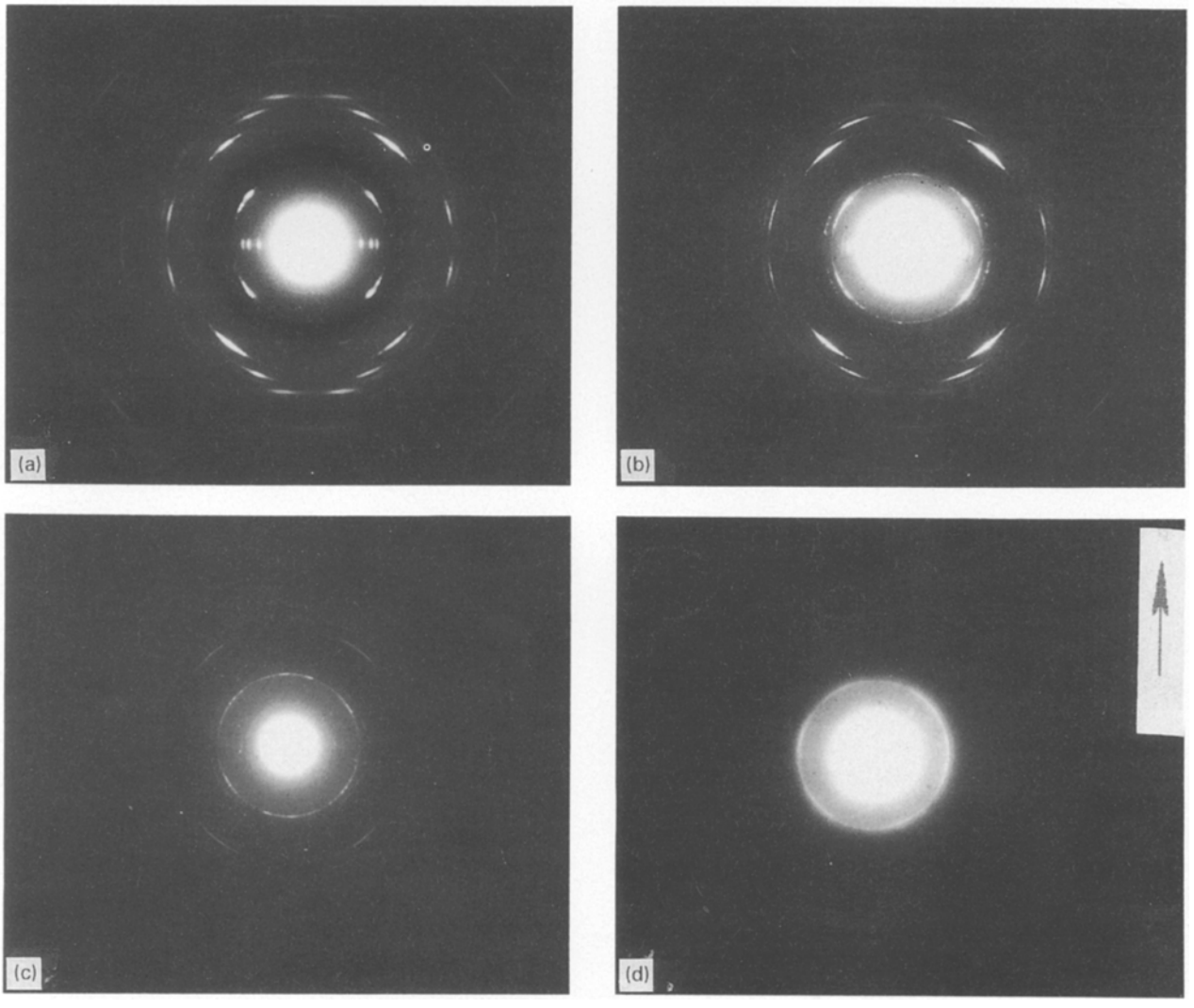

Figure 8 The corresponding electron diffraction patterns of HDPE-iPP multilayered films as in Fig. 7.

(0 2 0) reflection changes only slightly. No (0 2 0) diffraction ring is observed. If the HDPE layer is too thick, e.g. about 500 nm, the only reflection observed is a diffuse (1 1 0) Debye–Scherrer ring, while all of the other reflections, including the (0 2 0) reflection of HDPE, have been shaded (Fig. 8d).

Fig. 9 shows the electron micrographs of HDPE-iPP multilayered films heat treated at 150°C for 10 min and then quenched directly into ice–water (0°C). The thickness of the HDPE layers is 90 and 150 nm, respectively. The size of the HDPE lamellae and their epitaxial relationship with iPP crystals are similar to that shown in Fig. 7. However, the results of electron diffraction (Fig. 10) indicate that the (1 1 0) diffraction ring occurs when the thickness of the HDPE layer is about 150 nm (Fig. 10b). Thus the thickness of the critical epitaxial layer of HDPE at this cooling rate is not more than 150 nm.

The above results indicate that during the fast cooling process, the HDPE forms a crystalline structure of two layers only (Fig. 11). The first layer always consists of epitaxial lamellae of HDPE, while the second layer is spherulitic. Unambiguously, a fast crystallization rate, as in the case of quenching the samples into air at room temperature, results in the formation of a thick epitaxial layer of HDPE (about 250 nm), i.e. the large width of the HDPE lamellae along the direction of the *a*-axes. At the same time, the fast crystallization rate also results in the nucleation and growth of HDPE spherulites in the second layer, following the crystallization of the first layer. On the other hand, if the crystallization is too fast, as in the case of quenching the samples into ice–water (0 °C), the critical epitaxial layer thickness of HDPE (the thickness of the first layer) decreases to about 150 nm. This is because the nucleation rate is so fast that the HDPE in both the first and second layers crystallizes almost simultaneously. When the growth of crystals in the two layers occurs, the crystallization process is complete. This is the reason for the smaller thickness of the first-layer crystals which formed during too rapid cooling.

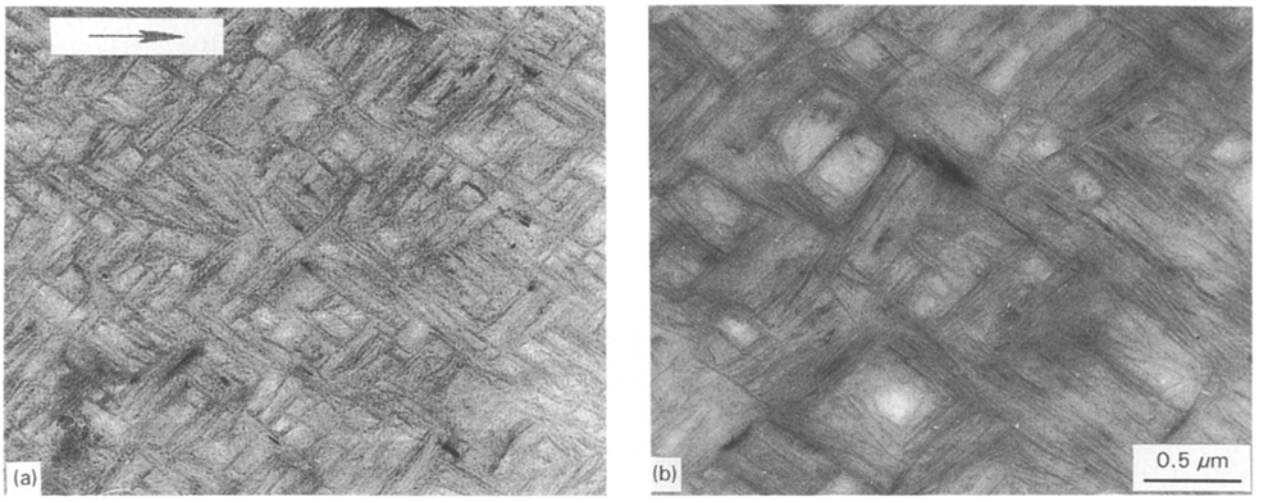

Figure 9 BF electron micrographs of HDPE-iPP multilayered films, heat treated at 150 °C for 10 min and quickly quenched into ice–water (0 °C). The thickness of the HDPE layer is (a) 120, and (b) 150 nm, respectively.

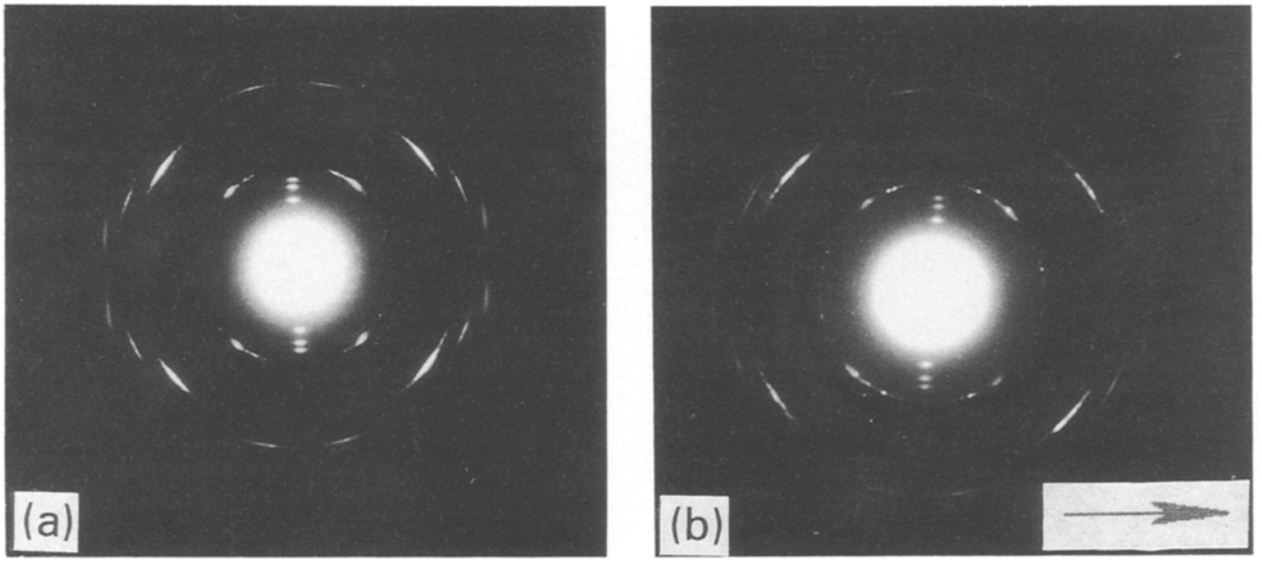

Figure 10 The corresponding electron diffraction patterns of HDPE-iPP multilayered films as in Fig. 9.

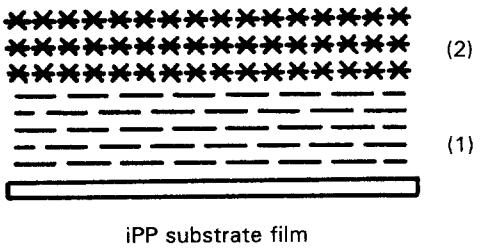

Figure 11 Model of crystallization of HDPE on iPP substrate film at high crystallization rates. (1) epitaxial HDPE layer, (2) HDPE spherulite layer.

4. Conclusion

Epitaxial nucleation and growth of HDPE on oriented iPP substrate take place only on the direct contact of HDPE with the surface of iPP. The thickness of the epitaxial interface layer or critical epitaxial layer of HDPE is strongly affected by the crystallization rate of HDPE. During a slow crystallization process, e.g. isothermal crystallization at 124 °C or slowly cooled at a rate of $\sim 0.5\,^{\circ}C\,min^{-1}$, the crystalline structure of three layers of HDPE, i.e. epitaxial lamellae (the first layer), oriented crystalline aggregates (the second layer) and spherulites (the third layer), are formed. The thickness of the critical epitaxial layer is about 100 nm. A fast crystallization rate results in the formation of a two-layer crystalline structure, i.e. epitaxial lamellae (the first layer) and spherulites (the second layer). The thickness of the critical epitaxial layer is about 250 nm for quenching into air at room temperature and 150 nm for quenching into ice–water.

Acknowledgements

The financial support from the Selected Research Program of Academia Sinica and the National Natural Science Foundation of China are gratefully acknowledged.

References

1. R. M. GOHIL, *J. Polym. Sci., Polym. Phys. Ed.* **29** (1985) 1713.
2. A. JABALLAH, V. RIECK and J. PETERMANN, *J. Mater. Sci.* **25** (1990) 3105.
3. I. HWA LEE and J. M. SCHULTZ, *ibid.* **23** (1988) 4237.
4. B. LOTZ and J. C. WITTMANN, *Makromol. Chem.* **185** (1985) 2043.
5. *Idem, J. Polym. Sci. Polym. Phys. Ed.* **24** (1986) 1559.
6. G. BROZA, V. RIECK, A. KAWAGUCHI and J. PETERMANN, *ibid.* **23** (1985) 2623.
7. J. PETERMANN and Y. XU, *J. Mater. Sci.* **26** (1991) 1211.
8. Y. SHEN, D. YANG and Z. FENG, *ibid.* **26** (1991) 1941.
9. B. GROSS and J. PETERMANN, *ibid.* **19** (1984) 105.
10. J. PETERMANN, G. BROZA, V. RIECK and A. KAWAGUCHI, *ibid.* **22** (1987) 1477.
11. J. C. WITTMANN and B. LOTZ, *J. Polym. Sci. Polym. Phys. Ed.* **23** (1985) 205.
12. J. PETERMANN and Y. XU, *Polym. Commun.* **31** (1990) 428.
13. J. PETERMANN, Y. XU and D. YANG, *ibid.* **33** (1992) 1096.
14. J. PETERMANN and R. M. GOHIL, *J. Mater. Sci.* **14** (1979) 2260.
15. D. YANG and E. L. THOMAS, *ibid.* **19** (1984) 2098.

Received 30 October 1992
and accepted 9 September 1993